Flow field characteristics of translating and revolving flexible wings

Yazdanpanah, Mahdi; Hazaveh, Hooman Amiri; Perçin, Mustafa; van de Meerendonk, Remco; van Oudheusden, Bas

Publication date
2019

Document Version
Final published version

Published in
10th Ankara International Aerospace Conference

Citation (APA)
Yazdanpanah, M., Hazaveh, H. A., Perçin, M., van de Meerendonk, R., & van Oudheusden, B. (2019). Flow field characteristics of translating and revolving flexible wings. In *10th Ankara International Aerospace Conference* Article AIAC 2019-177

10th ANKARA INTERNATIONAL AEROSPACE CONFERENCE AIAC-2019-177
18-20 September 2019 - METU, Ankara TURKEY

FLOW FIELD CHARACTERISTICS OF TRANSLATING AND REVOLVING FLEXIBLE WINGS

Mahdi Yazdanpanah[1], Human Amiri[2] and Mustafa Percin[3]
Middle East Technical University
Ankara, Turkey

Remco van de Meerendonk[4] and B.W. van Oudheusden[5]
Delft University of Technology
Delft, The Netherlands

ABSTRACT

This study explores the effects of rotational mechanisms on the characteristics of the leading edge vortex (LEV) by comparing translating and revolving flexible wings that are started from rest. Tomographic particle image velocimetry (tomographic-PIV) technique was employed to acquire three-dimensional flow fields for the revolving wings, while planar flow fields for the case of translating wings were acquired via 2D2C-PIV measurements. The comparison of flow fields between the two motion kinematics reveals similar behavior of the vortical structures yet the LEV circulation in the translating wings has higher values. The LEV centroid in the revolving cases stays above the leading edge, while in the translating wings, it always remains at a lower position. The effect of high flexibility results in the retention of LEV closer to the wing surface for both cases.

INTRODUCTION

The design and development of aerial vehicles have been inspired by nature for centuries. Recently, with the advent of micro air vehicles (MAVs), the flapping flight of biological flyers has been explored by many researchers at the typical low Reynolds number (Re) due to having better aerodynamic performance compared to fixed and rotary wings [Pines and Bohorquez, 2006].

The flow around the flapping wings is unsteady, where the generation of a stable leading edge vortex (LEV) has shown to be one of the most prominent force generation mechanisms [Sane, 2003].

The flapping wing motion can be decomposed into three motion kinematics: sweeping, plunging and pitching. In the literature, the sweeping motion is simulated by either a rectilinear translation (i.e., infinite Rossby number) or revolving motion (finite Rossby number). In 2-D translational motion, the flow separates at the wing leading edge, forming a LEV. If the wing travels more, the trailing edge vortex (TEV) sheds to the wing wake. This is followed by the growth of LEV. The LEV cannot remain attached, and it sheds to the wake. In contrast to translating motion, a stable LEV presents during the revolving motion [Sane, 2003]. Figure 1 represents a comparison between the flow around a wing in translating and revolving motions. Numerous studies and different hypotheses support the idea of presence of stable LEV in revolving motion such as spanwise

[1] Geaduate student in Department of Aerospace Engineering, Email: mahdi.yazdanpanah@metu.edu.tr
[2] Researcher at METU, Email: hamiri@metu.edu.tr
[3] Assistant Professor, Department of Aerospace Engineering, Email: mpercin@metu.edu.tr
[4] Researcher at ASML, Email:remcovandemeerendonk@gmail.com
[5] Associate Professor, Faculty of Aerospace Engineering, Email: b.w.vanoudheusden@tudelft.nl

advection of vorticity [Ellington et al., 1996], tip vortex inducing a downward flow and inhibiting the growth of the LEV [Birch and Dickinson, 2001] or the apparent rotational (Coriolis and rotational) accelerations in the low Rossby number regime [Lentink and Dickinson, 2009].

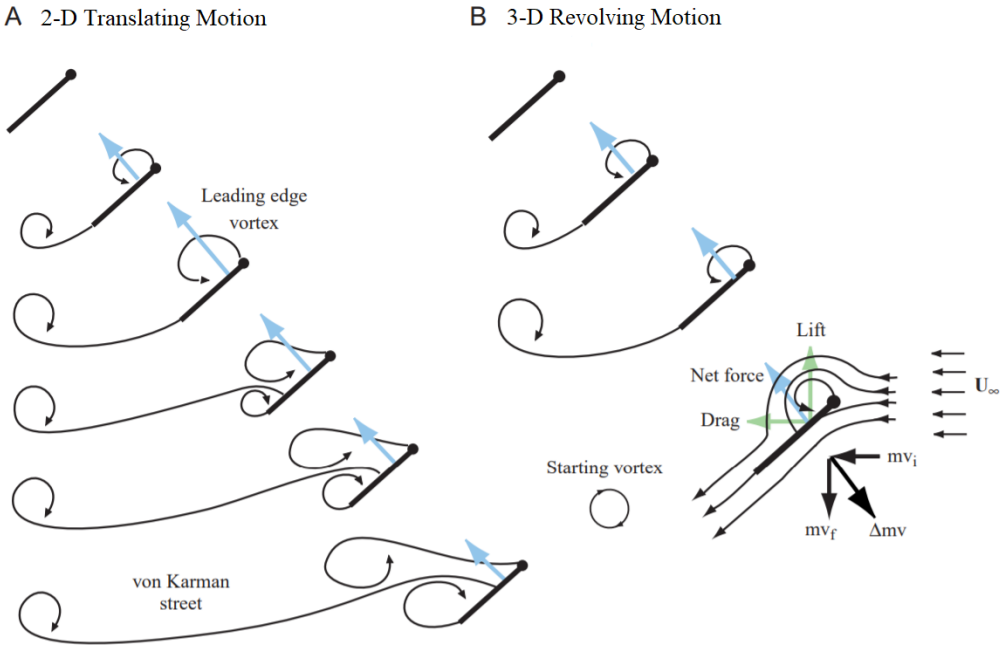

Figure 1: A comparison between translating and revolving motions [Sane, 2003]

Biological flyers in reality have flexible wings which is an aspect often disregarded in mechanical simulations. The presence of wing flexibility complicates the investigation of flapping-wing flight due to deformation of the wings in different maneuvers. Some studies on wing flexibility have shown the possible benefits of flexible wings on aerodynamic performance of flapping-wings [Shyy et al., 2010]. Zhao et al. [2010] showed that the flow structures are not changed by wing flexibility; however, the LEV size is smaller for flexible wings which agrees with the generation of aerodynamic forces; as the LEV size becomes smaller, the aerodynamic forces decrease. In the revolving case of the current study, the highly flexible wing had higher L/D which reveals the beneficial effects of flexible wings on aerodynamic performance of the wings in the sweeping motion (Figure 2).

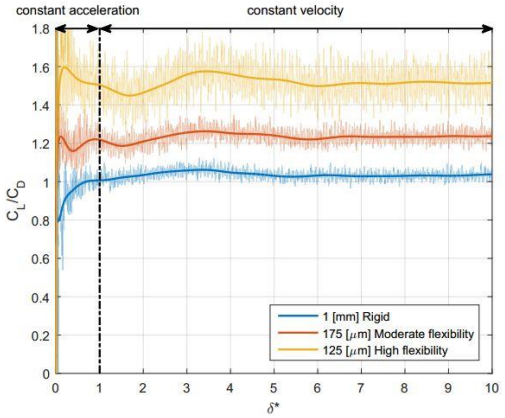

Figure 2: Temporal evolution of C_L/C_D for the studied revolving flat plates [van de Meerendonk, 2016]

The main objectives of this study are: (1) to investigate the effects of rotational mechanisms that are responsible for the stability of the LEV for chordwise-flexible wings by means of comparing two motion kinematics surging translational motion and surging revolving motion; (2) to investigate the effects of wing flexibility on the LEV and flow field characteristics.

For these purposes, three different flexural stiffness values (rigid, moderate flexibility and high flexibility) are considered. Force and tomographic particle image velocimetry (tomographic-PIV) measurements were performed on the revolving wings [van de Meerendonk et al., 2018]. Flow field measurements via 2D-PIV technique were conducted for the translating wings case.

EXPERIMENTAL SETUP

Both motion kinematics (revolving and translating) include an acceleration phase and a constant speed phase. The wing begins to revolve (translate) from rest, and it moves with constant acceleration until it reaches the predefined terminal velocity (V_t) over one chord length of travel ($\delta^*=1$), which for the revolving wing is measured at the 75% span location. Subsequently, the wing continues its motion at this velocity up to more than four chord lengths of travel. The value of V_t is 0.2 m/s for the revolving experiment and 0.08 m/s for the translating-wing experiments, the different values being a consequence of the different restrictions of the two setups. However, the wing dimensions are scaled accordingly in order to achieve equivalent values of the stiffness parameter.

Three wing models with different flexural stiffness values were considered for the tests. A virtually rigid wing is built from 1 mm thick Plexiglas, whereas the moderately flexible and highly flexible wings are built from Polyethylene terephthalate (PET) with thickness values of 175 μm and 125 μm, respectively. For the revolving wing experiments, the model is a rectangular flat plate with a chord length (c) of 50 mm and a span length of 100 mm, while for the translating wing experiments the model has a chord length (c) of 92 mm and a span length of 184 mm. In both cases, the wing aspect ratio is 2. The corresponding Reynolds number for the revolving and translating wing experiments are 10,000 and 7,360, respectively. The relative insensitivity of the flow structures to Reynolds number in this flow regime [Percin and van Oudheusden, 2015] allows for a proper comparison between the two tested motion kinematics. Bending stiffness parameter (Π), which describes the ratio between the elastic bending forces and the fluid-dynamic forces is as follows [Shyy et al., 2010]:

$$\Pi_1 = \frac{Eh^3}{12(1-\upsilon^2)\rho V_t^2 c^3}\ , \qquad (1)$$

where υ is the Poisson ratio, E is Young's modulus, h is thickness value, and V_t is terminal velocity. In the bending stiffness parameter equation, a Poisson ratio (υ) of 0.4 for Plexiglas and PET is considered. 1000 (kg/m^3) is taken for the density of water. The dimensions of translating wings are calculated to have the same stiffness parameters as the revolving wings have. The material properties of the wing models are reported in Table 1.

Table 1: Model properties

Material	Description	Young's modulus E $[Nm^{-2}]$	Thickness h [mm]	Bending stiffness parameter Π_1
Rigid	Plexiglas	$\approx 3300 \cdot 10^6$	1	65.5
Moderate flexibility	PET	$\approx 4350 \cdot 10^6$	0.175	0.46
High flexibility	PET	$\approx 4500 \cdot 10^6$	0.125	0.17

The revolving-wing experiments were performed in an octagonal water tank (Figure 3) at the Aerodynamics Laboratory of Delft University of Technology (TUD) [van de Meerendonk et al., 2018]. The translating wing experiments were performed in an octagonal water tank at the Aerospace Engineering Department of Middle East Technical University (METU). The dimensions of the tank are 1 m × 1.5 m (distance between parallel edges × height) and the wing models are driven in the tank by a robotic arm having three degrees of freedom (translation in the x and y-axes and 360° of rotation around the pitching axis of the wing model). PIV cameras are placed on the camera board, which is connected to robotic arm, and it moves with the robotic arm. Thus the flow field and leading edge positions in all images are same. Experimental setup for the translating-wing experiments is shown in Figure 4. The 2D-PIV setup is composed of a double-pulse Nd: YAG laser at a wavelength of 532 nm with a pulse energy of 120 mJ and two 12-bit HiSense MkII CCD cameras placed side-by-side in order to increase the field of view to 247.5 mm × 143.9 mm. The corresponding magnification factor is 0.059. The PIV Images from two cameras were stitched according to the mapping information obtained before the PIV measurements. The double-frame images were cross-correlated using interrogation areas of 64 × 64 $pixel^2$ with 75% of overlap. The universal outlier detection technique [Westerweel and Scarano, 2005] was applied to the cross-correlation results to detect and substitute the unreliable velocity vectors. Finally, for each phase the velocity fields were ensemble averaged in order to increase the signal to noise ratio.

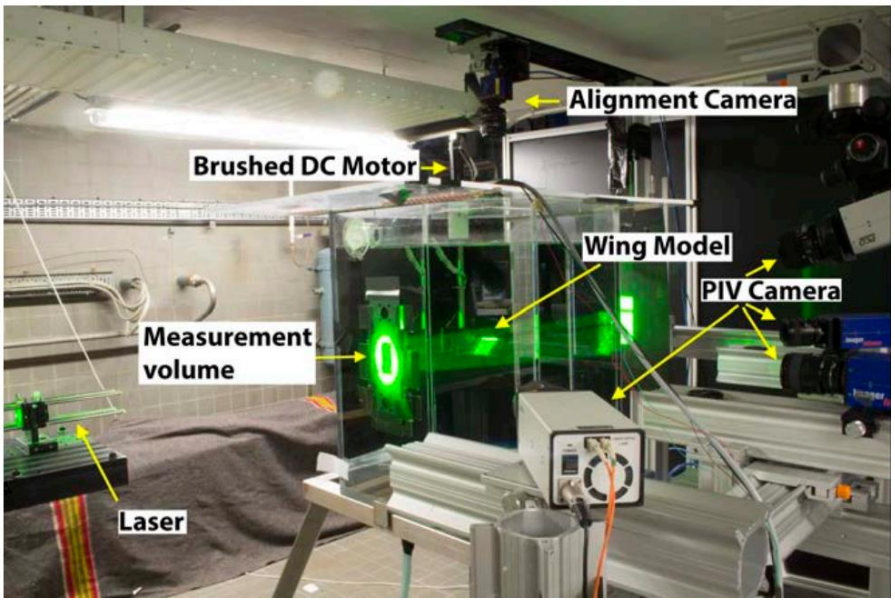

Figure 3: Tomographic PIV setup for revolving-wings experiments.

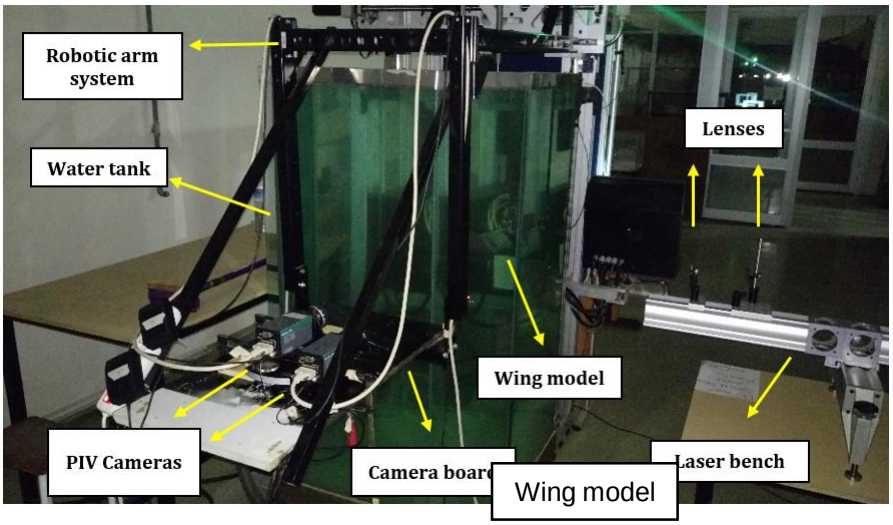

Figure 4: 2D-PIV setup for translating-wing experiments.

RESULTS

When the wings start to move, the rigid wing has a constant angle of attack during the motion, whereas the flexible wings deform during the translation which results in changing of angle of attack. The geometric angle of attack can be defined as the angle between the wing motion direction and the line connecting the leading edge and trailing edge. It is put forward by van de Meerendonk [2016] that the resultant force direction for the revolving flexible wings is normal to the line connecting leading edge to the trailing edge in the deformed state as shown in Figure 5. This is basically due to the dominance of the pressure forces which are generated due to the low-pressure region formed by the leading edge vortex.

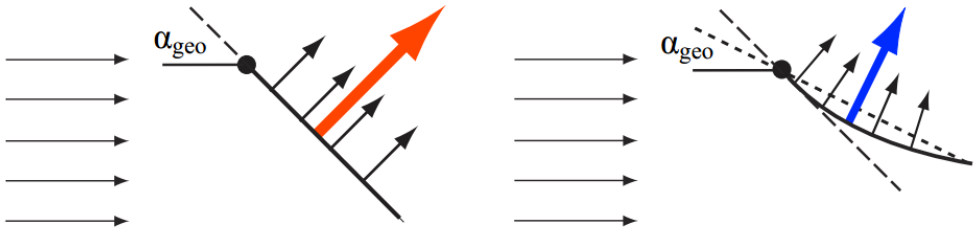

Figure 5: Schematic of net force acting on the wing and geometric angle of attack. Left: Rigid wing. Right: Flexible wing. Small vectors show the local net forces along the chord and the big vectors represent the resultant net force [van de Meerendonk, 2016]

It was shown by van de Meerendonk [2016] that there was a linear twist in revolving wings, thus weighted average of root and tip geometrical angle of attack in revolving wings with respect to 75% of span position was calculated for proper comparison with that of the translating wings. The temporal evolution of geometric angle of attack for translating flexible wings at 75% of span position, and weighted average of tip and root geometric angle of attack in revolving flexible wings are shown in Figure 6.

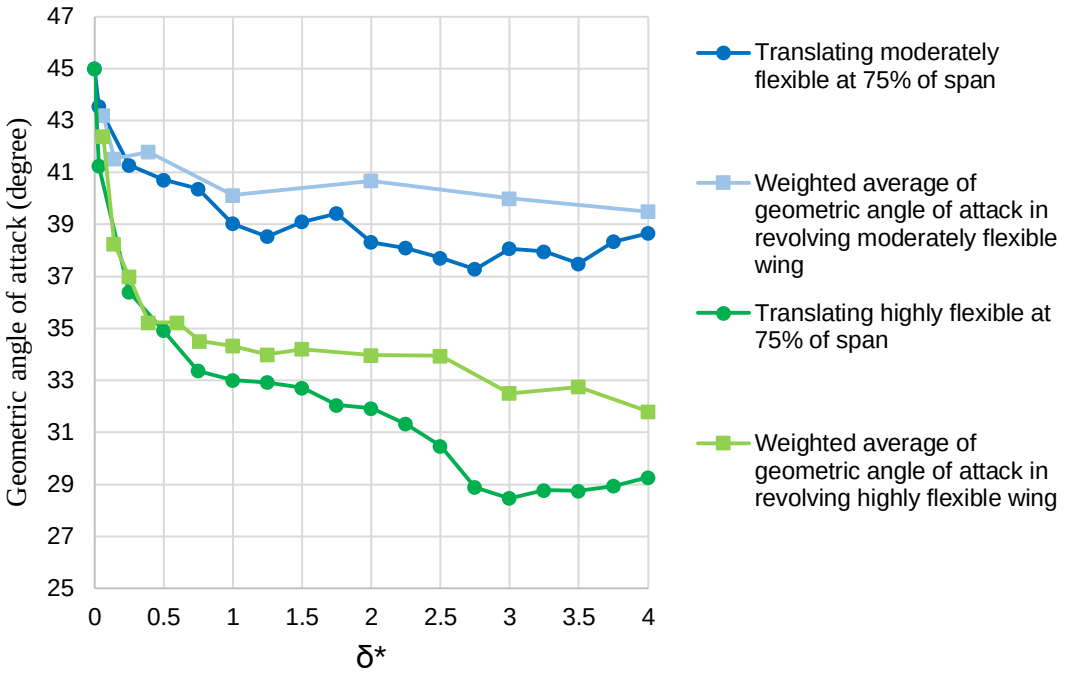

Figure 6: Temporal evolution of geometric angle of attack for translating flexible wings and weighted average of tip and root geometric angle of attack for revolving flexible wings

It is clear that the highly flexible wing deforms more than the moderately flexible one and presumably the force vector is tilted more towards the lift direction due to relatively lower geometric angle of attack. The comparison between the geometric angle of attack in both cases reveals that the geometric angle of attack in translating flexible wings is smaller than that of the revolving flexible wings. In the revolving wings, the wing tip deforms more than the wing root due to nature of the revolving motion and thus variation of the fluid forces along the span. The average difference of geometric angle of attack between two motion kinematics in moderately flexible and highly flexible wings during constant velocity phase are 1.5 and 2.4 degrees, respectively.

The out-of-plane vorticity contours at the 75% span position for δ^*= 1.0, 1.5, 2, and 4 for the translating and revolving flexible wings are shown in Figure 7, respectively. The out of plane vorticity contours suggest similar vortex formations: a coherent LEV and a train of trailing edge vortices particularly at the initial phases of both motion kinematics and a chaotic flow field with an elongated incoherent positive vorticity layers emanating from the leading edge at a later phase (δ^*= 4). At the end of the acceleration phase for both motions (δ^*= 1), a lifted off fragmented LEV is present in the flow fields, which is in accordance with those reported in the literature [Percin and van Oudheusden, 2015]. In the subsequent stages, the behavior of the LEV is similar for both motion kinematics, yet the LEV circulation value is slightly higher in the case of the translating wing, as shown in Figure 8. At δ^*= 4, the coherent LEV is burst into small-scale structures in both translating and revolving wings. Particularly in the case of rigid and moderately flexible wings, the shear layers emanating from the leading and trailing edges interact, and this interaction leads to small-scale vorticity pockets populating the wake. For the translating rigid and moderately flexible wings, the flow is completely detached from the wing surface, however, for the highly flexible wing, the flow that separates at the leading edge reattaches to the wing surface slightly before the trailing edge. This may be attributed to the decreased geometric angle of attack of the highly flexible wing due to relatively higher deformation.

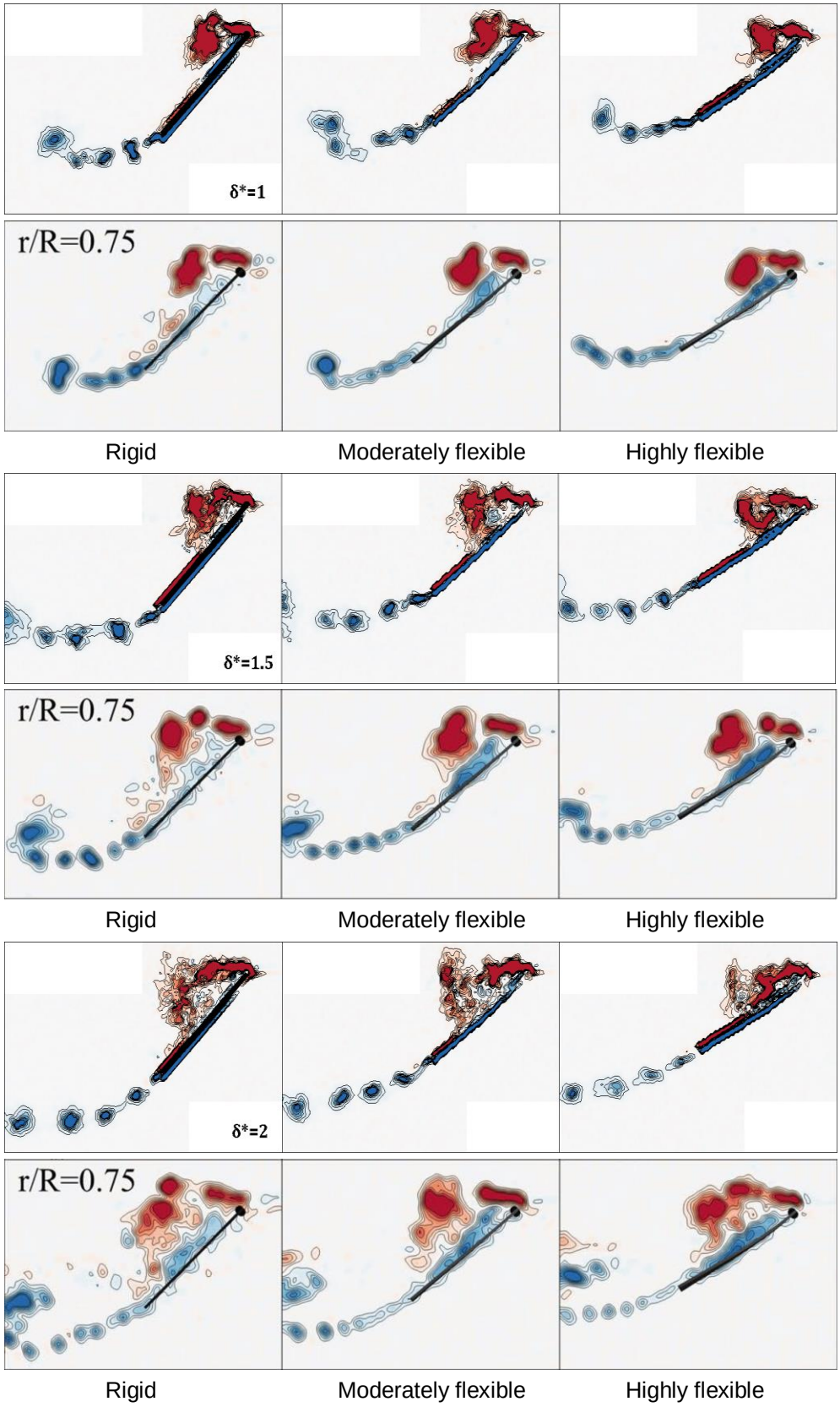
Translating wings
δ*=1
Revolving wings
r/R=0.75
Rigid
Moderately flexible
Highly flexible
Translating wings
δ*=1.5
Revolving wings
r/R=0.75
Rigid
Moderately flexible
Highly flexible
Translating wings
δ*=2
Revolving wings
r/R=0.75
Rigid
Moderately flexible
Highly flexible

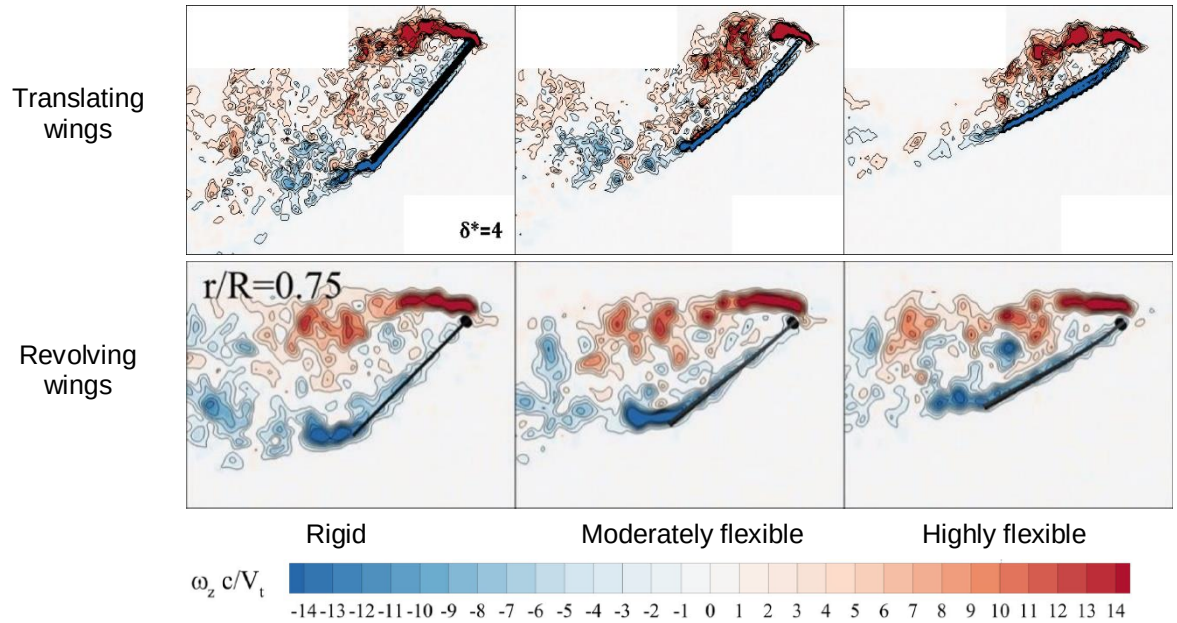

Figure 7: The out-of-plane vorticity contours for δ*=1.0, 1.5, 2 and 4 with respect to the 75% span position. First row: Translating wings. Second row: Revolving wings.

There are two prominent differences between the translating and revolving wings in terms of the normalized LEV circulation values. First, the translating motion yields greater circulation values. Second, the LEV circulation stays higher after δ*= 3 compared to the revolving wing case. However, this may be due to the shortcoming of the vortex core detection strategy in the detection of the LEV boundaries.

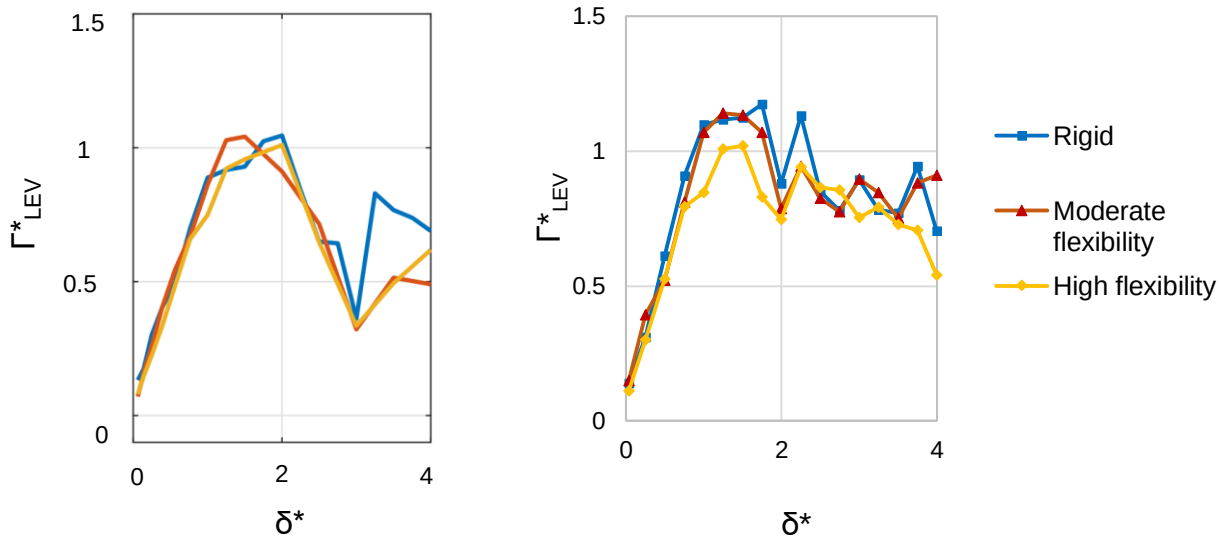

(a) Revolving (b) Translating

Figure 8: Temporal evolution of LEV circulation (Γ^*_{LEV}) for translating and revolving wings.

According to the Kelvin's circulation theorem, the circulation around a closed curve moving with the fluid remains constant with time ($D\Gamma/Dt = 0$) [Anderson, 2011]. Trailing edge vortex circulation is calculated for the initial stages of the translation motion ($\delta^* \leq 1.25$) in order to compare with the LEV circulation values. Such a comparison may allow for assessing the presence of the bound circulation under the assumption of two-dimensional flow around the wings at the early stages [Percin and van Oudheusden, 2015]. In an earlier study, Pitt Ford and Babinsky [2013] showed that most of the circulation is contained in the LEV and the bound circulation remains small for a translating flat-plate airfoil at a fixed angle of attack of 15°. Percin and van Oudheusden [2015] also reported a similar behavior for a revolving flat-plate wing at an angle of attack of 45°. Comparison of the LEV and TEV circulation values (Figure 9) suggests that there has to be a bound circulation or another source of circulation in the same sense with the TEV for the Kelvin's circulation theorem to be satisfied. This major difference may also be due to three-dimensionality of the flow even at early stages of the motion. Note that, in order to allow for a proper comparison, the LEV circulation values are multiplied by -1

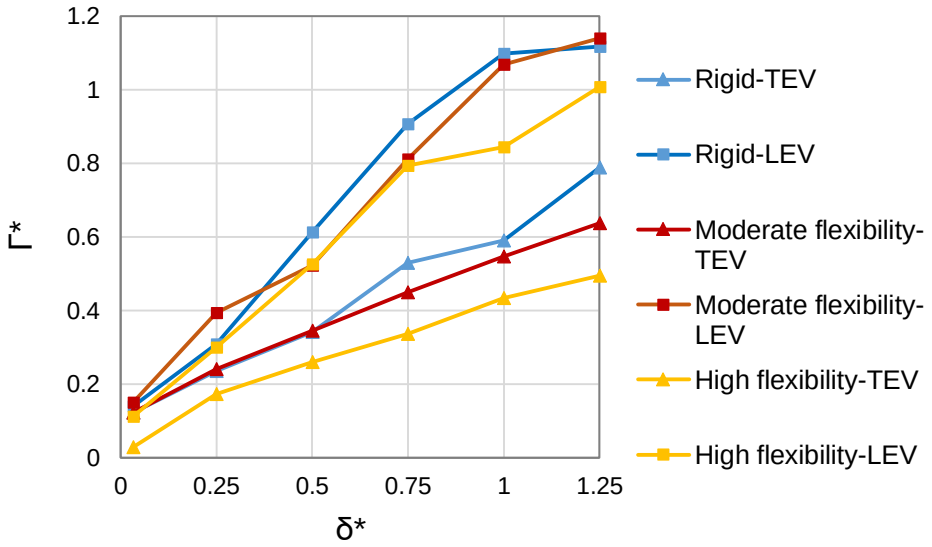

Figure 9: Temporal evolution of LEV circulation (Γ^*_{LEV}) and TEV circulation (Γ^*_{TEV}) in initial stages of motion (note that the LEV circulation values are multiplied by -1 to facilitate the comparison).

The temporal evolution of the LEV centroid in x and y directions (Figure 10) displays a similar trend for both motion kinematics. The major difference in this respect is that the LEV stays at a lower location (y/c) with respect to the leading edge and continuously move away in the vertical direction in the case of the translating wing while it stays at a more-or-less fixed location in the case of the revolving wing. The LEV rises and stays at a higher position with respect to the leading edge in the revolving wings, while in the translating wings, it always stays at a relatively lower position.

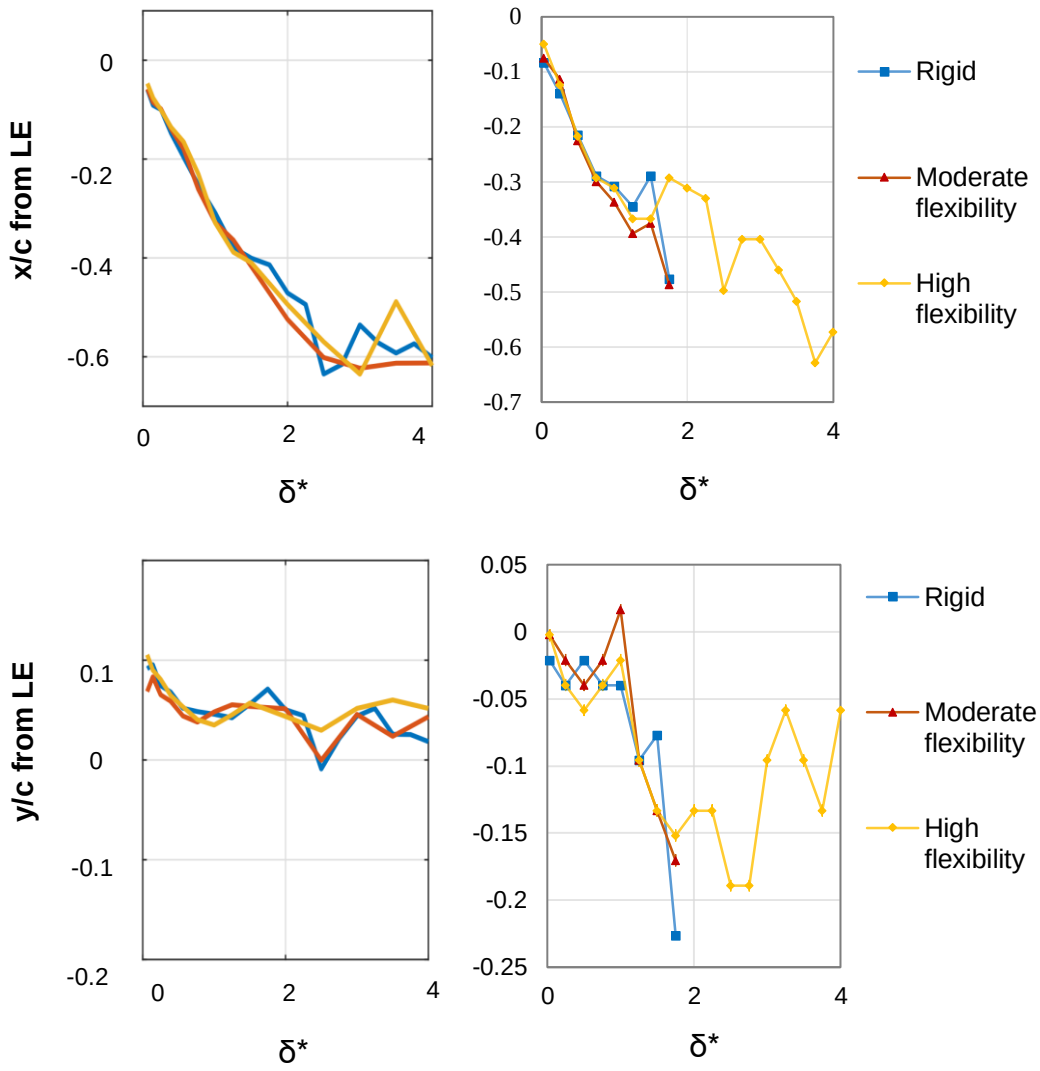

(a) Revolving (b) Translating

Figure 10: Temporal evolution of the LEV centroid. Top: Chord distance in x-direction from LE. Bottom: Chord distance in y-direction from the LE.

Temporal evolution of LEV centroid normal distance from the wing surface (s/c) for translating and revolving wings is shown in Figure 11. In both cases, the LEV stays closer to the wing surface in the case of the highly flexible wing. This may also boost force production due to the associated low pressure region [van de Meerendonk et al., 2018]. However, it should also be noted that the LEV circulation and hence the magnitude of the associated low-pressure region is relatively low for the highly flexible wing due to decreased geometric angle of attack.

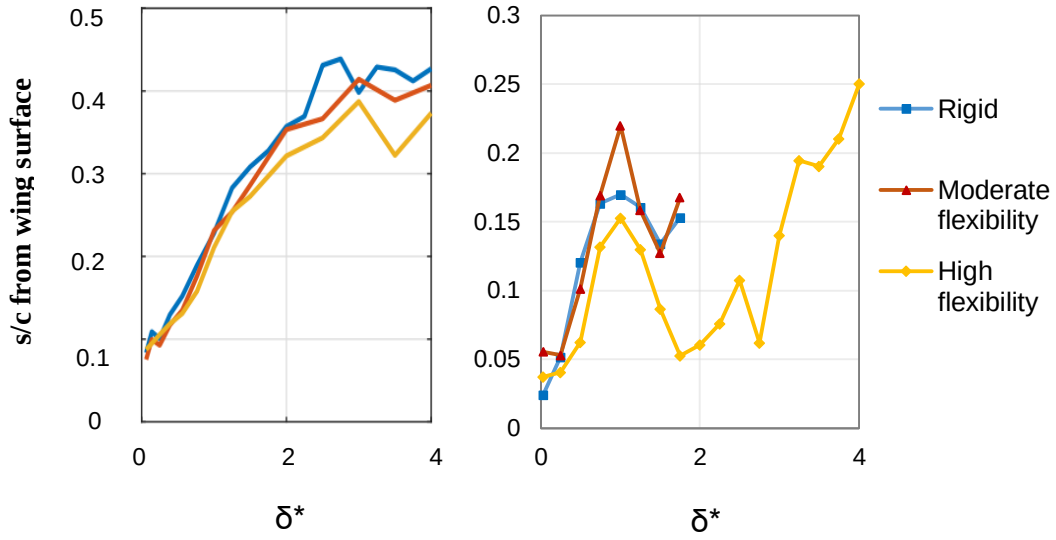

(a) Revolving (b) Translating

Figure 11: Temporal evolution of LEV centroid distance from the wing surface. Left: Revolving wings. Right: Translating wings.

CONCLUSIONS

The flow characteristics of rigid and flexible wings undergoing revolving and translating motions were investigated in this study. Three-dimensional flow fields were acquired by the use of tomographic-PIV for the revolving wings and planar flow fields were studied by employing 2D2C PIV for the translating wings. LEV characteristics in both motion kinematics was explored. The comparison of geometric angle of attack in the translating flexible wings reveals that the highly flexible wing deforms more than the moderately flexible one and presumably the force vector is tilted more towards the lift direction due to relatively lower geometric angle of attack. The comparison between the geometric angle of attack in translating and revolving wings (see Figure 6) reveals that the geometric angle of attack at 75% of span position of translating wings is smaller than that of the revolving wings. This is attributed to smaller deformation of the revolving wing associated with the curvilinear nature of the motion.

The comparison between the results of this study with the revolving wings study revealed that the vortex structures have similar behavior in the acceleration phase of both cases. In the subsequent stages, the wings have similar chaotic flow in the wake in both cases; however, the highly flexible wing in the translating motion generates less chaotic flow due to the reattachment of the flow which leaves the TE tangentially. In the translating rigid and moderately flexible wings, the flow cannot reattach completely to the wing surface and the LEV sheds to the wake.

The LEV circulation was shown that is a slightly higher in the translating cases comparing to the revolving wings. This may be due to rotational accelerations that plays role in the convection of vorticity in the spanwise direction in the revolving wings. The LEV circulation drops in the translating wings after $\delta^*=1.75$ and in the revolving wings after $\delta^*=2$; however, it stays higher after $\delta^*=3$ in the translating cases.

The comparison of the LEV and TEV circulation values in translating wings shows that there has to be another source of circulation or a bound circulation in the same sense with TEV for the Kelvin's circulation theorem to be satisfied. The three-dimensionality of the flow in the translating motion even at initial stages of motion can be the reason of this difference.

The LEV centroid positions are similar for all wings in the acceleration phase, and they follow different path in the constant velocity phase of motion. The vortex centroid detection method showed that the LEV is burst in the rigid and moderately flexible wings undergoing the linear translating motion after 1.75 chords traveled and cannot be detected; however, the LEV in the highly flexible wing keeps its coherency due to the deflection of the wing, and thus smaller geometric angle of attack. The result of this study showed that the effect of high flexibility mediates the LEV.

In both revolving and translating highly flexible wings, the LEV remains close to the wing surface which may result in force production enhancement due to associated lower pressure region. Decrease in geometric angle of attack results in lower LEV circulation and the magnitude of the associated low-pressure region which also has an effect on the force production

References

Anderson, J. (2011) *Fundamentals of Aerodynamics*, Anderson series, McGraw-Hill

Beals N, and Jones AR (2015) *Lift Production by a Passively Flexible Rotating Wing*, *AIAA Journal* 53:10

Birch JM, and Dickinson MH (2001) *Spanwise flow and the attachment of the leading-edge vortex on insect wings*, Nature 412:6848

Ellington CP, Van Den Berg C, Willmott AP, and Thomas AL (1996) *Leading-edge vortices in insect flight*. Nature 384:6610

Jardin T, and David L (2014) Spanwise gradients in flow speed help stabilize leading-edge vortices on revolving wings, Physical Review E 90:1

Jardin T, and David L (2015) *Coriolis effects enhance lift on revolving wings*, Physical Review E 91:3

Lentink D, and Dickinson MH (2009) *Rotational accelerations stabilize leading edge vortices on revolving fly wings*, Journal of Experimental Biology 212:16

Percin M, and van Oudheusden BW (2015) *Three-dimensional flow structures and unsteady forces on pitching and surging revolving flat plates*, Experiments in Fluids 56:47

Pines DJ, and Bohorquez F (2006) *Challenges Facing Future Micro-Air-Vehicle Development*, Journal of Aircraft 43:2

Pitt Ford CW, Babinsky H (2013) *Lift and the leading-edge vortex*, Journal of Fluid Mechanics 720, 280-313

Sane SP (2003) *The aerodynamics of insect flight*. Journal of Experimental Biology 206:23

Shyy W, Aono H, Chimakurthi SK, Trizila P, Kang CK, Cesnik CE, and Liu H (2010) *Recent progress in flapping wing aerodynamics and aeroelasticity*, Progress in Aerospace Sciences 46:7

Van de Meerendonk, R (2016). Three-dimensional flow and load characteristics of flexible revolving wings at low Reynolds number. Master thesis, Delft University of Technology.

van de Meerendonk R, Percin M, and van Oudheusden BW (2018) *Three-dimensional flow and load characteristics of flexible revolving wings*, Experiments in Fluids 59:161

Westerweel J, and Scarano F (2005) *Universal outlier detection for PIV data*, Experiments in Fluids 39: 1096

Zhao L, Huang Q, Deng X, and Sane SP (2010) *Aerodynamic effects of flexibility in flapping wings*, Journal of The Royal Society Interface 7:44